Wetting behavior of H_2 on cesium

D. Ross,* P. Taborek, and J. E. Rutledge

Department of Physics and Astronomy, University of California, Irvine, California 92697-4575

(Received 8 June 1998)

We have studied the wetting behavior of H_2 on Cs by measuring contact angles and adsorption isotherms as functions of the temperature. These measurements were made on the same Cs surface and they quantitatively determine the parameters needed to model the wetting behavior in this system. We find that the wetting temperature for H_2 on Cs is 20.57 ± 0.05 K and the coefficient of the van der Waals attraction is $2700 \pm 300 K$ Å^3. The data are inconsistent with the usual assumption that the surface tensions at the solid interface are temperature independent. [S0163-1829(98)52432-0]

Over the last several years new systems have become available for studies of wetting transitions, namely cryogenic liquids on the surfaces of alkali metals. Most experimental studies have involved liquid helium, but H_2 on Rb (Refs. 1 and 2) and Ne on Rb and Cs (Ref. 3) have also been investigated. These systems offer some significant experimental advantages over more traditional ones which utilize organic liquids. These include extreme cleanliness and relatively short thermal and mass equilibration times. As a result, several wetting phenomena that had existed only in theory were experimentally realized for the first time in these systems. The interplay between theory and experiment in studies of the new wetting systems has been remarkably vigorous. Indeed, the field stemmed from a theoretical prediction[4] and many of the experimental results have been anticipated by explicit, quantitative theoretical predictions.[5] Quantitative theories are possible because the interactions between the adsorbates and the alkali metals are relatively simple and well known. Consequently, quantitative experiments are of interest.

We present here studies of the wetting behavior of liquid H_2 on the surface of Cs. Above the wetting temperature, T_w, we have measured adsorption isotherms to locate the prewetting line. Below the wetting temperature isolated droplets can be formed. We have used optical imaging of the droplets to measure the contact angle as a function of temperature. The combination of these two measurements is required to constrain the parameters that determine the location of the prewetting line; both measurements have been made on the same surface. The results include quantitative measurements of T_w and the van der Waals interaction strength between the H_2 and a Cs surface. The measurements show that the temperature dependence of surface tensions at the liquid-solid interface are not negligibly weak as has been assumed.[1,2,6]

The experimental techniques we used are similar to those we have employed to study wetting of helium on Cs.[7–9] The Cs surfaces were prepared by evaporating 40 monolayers of Cs from a resistively heated oven containing pure Cs metal onto both sides of a quartz microbalance. During the evaporation, the cell containing the quartz microbalance was held below 6 K to eliminate contamination. After evaporation, the microbalance was heated to about 80 K and held there for 30 min, while the rest of the cell was again maintained at low temperature. To measure adsorption isotherms, small doses of ultrapure H_2 gas were admitted to the cell through a heated fill tube. As the H_2 adsorbed on the surface, the resonant frequency of the microbalance shifted lower by an amount Δf, which is proportional to the areal mass density of the adsorbed hydrogen. The proportionality constant is 0.125 Hz/H_2 layers. The contact angles were measured on exactly the same surface used in the adsorption isotherm experiments. A capillary was placed about 0.5 mm above the surface of the microbalance. H_2 gas was metered into the capillary where it liquified and dripped onto the surface. Sufficient time for ortho-para conversion was not allowed. Consequently the H_2 in the experiment was ''normal'' H_2, 75% o-H_2 and 25% p-H_2. As more liquid was forced through the capillary the droplet grew and the contact line of the droplet slowly moved radially outward from the capillary. A digital camera and a long focal length microscope were used to photograph the droplet through infrared radiation absorbing windows. The advancing contact angle, which is known to be equal to the thermodynamic contact angle for all but the most heterogeneous surfaces,[10] was determined from the digital images. Liquid could also be removed from the droplet and the receding contact angle determined. Contact angle hysteresis on these surfaces was small. The receding contact angle was only $5° \pm 2°$ smaller than the advancing angle across the temperature range from just above the triple point temperature to the wetting temperature. Inspection of the images shows that our Cs surfaces were smooth and free of defects larger than a few microns. It is interesting to note that the contact angle for ^{4}He on the same Cs surface showed the same large hysteresis is described in Ref. 8.

Figure 1 shows an advancing contact angle measurement at 16.6 K. The optical axis of the microscope is inclined a few degrees above the Cs surface. Because the substrate is reflective, both the free surface of the H_2 droplet and its reflection in the Cs surface are visible. The sharp points, where the surface and its reflection meet at the edge of the droplet, lie on the Cs surface. The 0.4 mm capillary can be seen protruding from the droplet. The contact angle is half of the angle between lines drawn tangent to the free surface and its reflection at the edge of the droplet.

Figure 2 shows the temperature dependence of the contact angle, θ. The error bars are $\pm1°$ and are due largely to uncertainties in the construction of the tangent lines. Young's
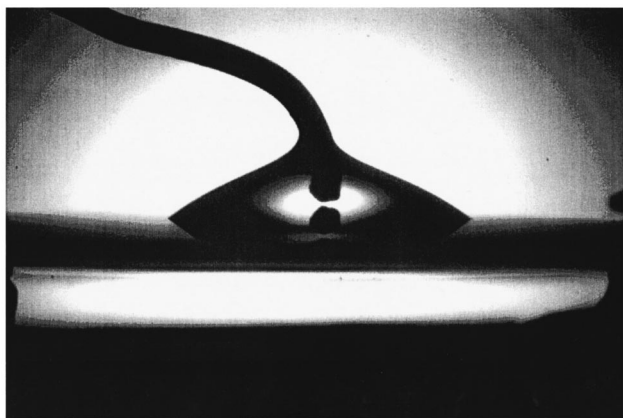
FIG. 1. A hydrogen droplet on a Cs surface. The droplet is viewed at grazing incidence so that the free surface and its reflection are seen. The dark object protruding from the top of the droplet is a 0.4-mm diameter capillary.

equation gives a simple relationship between the contact angle and the interfacial surface tensions,

$$\sigma_{lv}\cos(\theta) = \sigma_{sv} - \sigma_{sl} \equiv \delta\sigma_s . \tag{1}$$

Here, σ_{lv}, σ_{sv}, and σ_{sl} are the liquid-vapor, solid-vapor, and solid-liquid surface tensions, respectively. The thermodynamic properties of liquid hydrogen, including σ_{lv}, are well known.[11] If one assumes that $\delta\sigma_s$ is temperature independent, the contact angle can be calculated from Eq. (1). The dashed curve in Fig. 2 shows the result, assuming T_w is 20.4 K. The dashed curve is a poor fit to the data and other choices of T_w are equally unsuccessful. It is immediately clear that $\delta\sigma_s$ is temperature dependent.

Equation (1) can be used to extract the temperature dependence of $\delta\sigma_s$ from the contact angle data. The data points in Fig. 3 show the result. For comparison, the dotted line shows σ_{lv}, which is remarkably linear in T over the entire range of our experiment. The data are consistent with the assumption that $\delta\sigma_s$ is also linear in T, as shown by the solid straight line in Fig. 3. The temperature dependence of $\delta\sigma_s$ is about a third as strong as the temperature dependence of σ_{lv}.

The high-pressure regions of three adsorption isotherms above T_w are shown in Fig. 4. The circles, squares, and dia-

FIG. 3. $\delta\sigma_s$ as a function of T. The dashed line shows σ_{lv} for comparison and the solid line is the best fit to the data.

monds are data taken at 24, 23, and 21.3 K respectively. During the experiment, the frequency shift was measured as a function of the pressure. In Fig. 4 we have plotted the frequency shift as a function of $\Delta\mu$, the difference between the chemical potential and the chemical potential at liquid-vapor coexistence. All three isotherms have the same shape. At low $\Delta\mu$, less than half a monolayer of H$_2$ is adsorbed and the isotherms are flat. As $\Delta\mu$ is increased, a sharp step appears in the isotherms. The position and height of the step vary with temperature. Above this step the adsorbed mass smoothly increases and diverges at liquid-vapor coexistence, $\Delta\mu = 0$. Similarly shaped isotherms have been measured for ^{4}He on Cs (Ref. 7) and H$_2$ on Rb (Refs. 1 and 2) and are clearly understood. At lower temperatures the abrupt increase in mass marks a prewetting transition, an extension of the wetting transition into the region of the bulk phase diagram where the vapor phase is stable. At the prewetting transition, thin and thick unsaturated films coexist. The locus of points in the $\Delta\mu$-T plane where prewetting occurs is a line of first-order surface transitions which ends in a prewetting critical point T_c^{PW}. However, the character of the isotherms above and below T_c^{PW} is only subtly different.[2,7] The step does not disappear but becomes a two-dimensional (2D) compressibility maximum that persists to temperatures much higher than T_c^{PW}. The prewetting data for H$_2$ on Cs are
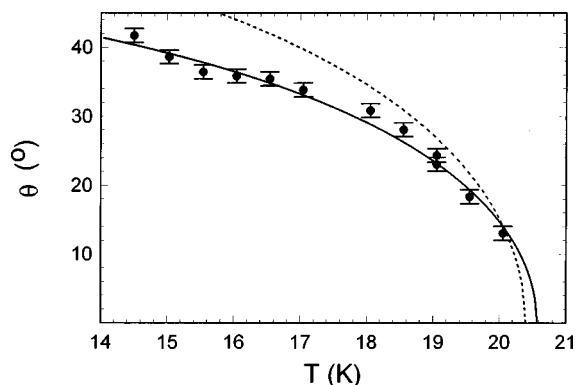

FIG. 2. The data points are from the analysis of images like that shown in Fig. 1. The dotted line is an attempt to fit the data with a temperature independent $\delta\sigma_s$. The solid line results from fitting procedure with a linearly T dependent $\delta\sigma_s$.
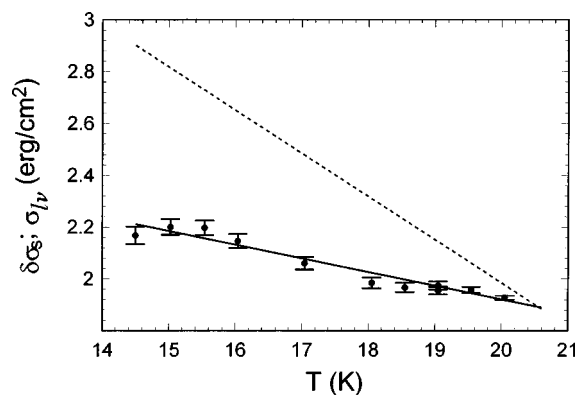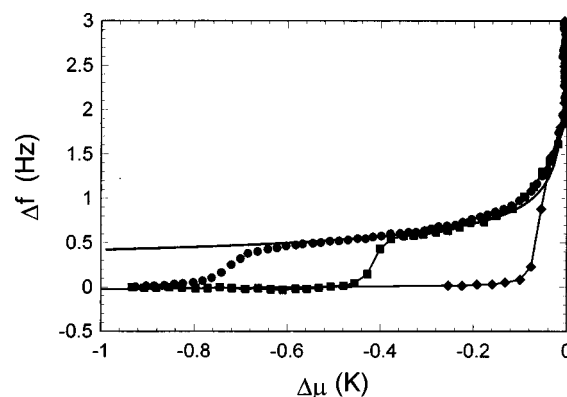

FIG. 4. Δf as a function of $\Delta\mu$. The circles are measured at 24 K, the squares at 23 K, and the diamonds at 21.3 K. The steps are due to prewetting. The solid curve through the data above the prewetting steps is the prediction using the value of ΔC_3 from the fitting procedure.
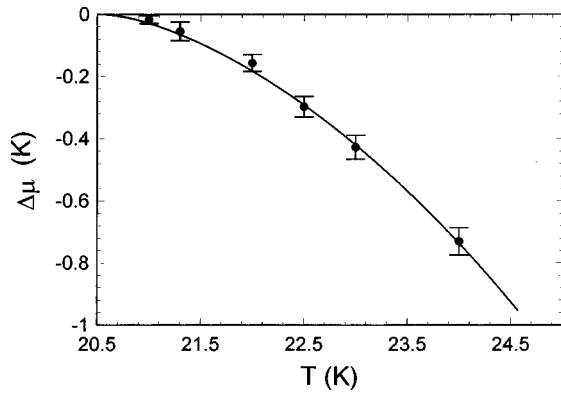
FIG. 5. The prewetting line in the $\Delta\mu$-T plane. The data points are from isotherms like those in Fig. 4. The solid line is the fit to the data.

shown in Fig. 5. The values of $\Delta\mu$ in the center of the abrupt rises establish the data points in Fig. 5 and the error bars span the width of the step.

For the case of temperature independent $\delta\sigma_s$, a model that predicts the location of the prewetting line has been developed.[1,2,6] It is easily generalized to include the temperature dependence of $\delta\sigma_s$. The result is

$$\Delta\mu_{\mathrm{PW}}(T) = -\left(\frac{2[\delta\sigma_s(T) - \sigma_{l\nu}(T)]}{3(\rho_l - \rho_\nu)(\Delta C_3)^{1/3}}\right)^{3/2}. \quad (2)$$

In Eq. (2), ρ_l and ρ_ν are the densities of the bulk liquid and vapor and $\Delta C_3 \equiv C_3^{\mathrm{Cs}} - C_3^{\mathrm{H}_2}$, where the C_3's are the coefficients of the van der Waals potentials between an H_2 molecule and a semi-infinite slab of Cs or bulk H_2.

Equation (2) shows that the location of the prewetting line depends on $\delta\sigma_s(T)$. Above T_w, however, the contact angle experiment cannot be done and no direct determination of $\delta\sigma_s(T)$ is possible. Since $\sigma_{l\nu}$ remains linear in T even up to 24 K, the highest temperature at which we measured adsorption isotherms, we shall assume that $\delta\sigma_s$ does also. It is clear that this assumed linearity must break down at some temperature because the extrapolation of the straight line shown in Fig. 3 does not pass through $\delta\sigma_s = 0$ near the bulk liquid-vapor critical temperature. It will be apparent if the assumption fails in the temperature range of the prewetting line

measurements because if it does, it will be impossible to fit Eq. (2) to the data of Fig. 5 with a constant value of ΔC_3. Because $\delta\sigma_s = \sigma_{l\nu}$ at T_w, it is convenient to parametrize $\delta\sigma_s$ as

$$\delta\sigma_s(T) = \sigma_{l\nu}(T_W) + \alpha(T - T_W). \quad (3)$$

With the further assumption that $\delta\sigma_s$ does not change substantially between coexistence and $\Delta\mu$ at prewetting, the prewetting line data and contact angle data are sufficient to determine, T_W, α, and ΔC_3.

A standard χ^2 analysis[12] simultaneously using the data from the contact angle and prewetting line experiments was used to select the best values and probable errors of T_W, α, and ΔC_3. χ^2 was constructed by summing the squares of the error-normalized deviations between the data in Figs. 3 and 5 and the predictions of Eq. (2) for the prewetting data or Eq. (3) for $\delta\sigma_s$. The fitting procedure gave $T_W = 20.57 \pm 0.05$ K, $\delta\sigma_s = (2.97 \pm 0.05) - (0.053 \pm 0.003)T$ erg/cm^2, and $\Delta C_3 = 1800 \pm 300$ K Å^3. The contact angles, values of $\delta\sigma_s$, and prewetting line calculated from the fit parameters are shown as solid lines in Figs. 2, 3, and 5. The quality of the fit apparent in Fig. 5 confirms the linearity in T of $\delta\sigma_s$ between T_w and 24 K. It is interesting to note that because the numerator in Eq. (2) and $\sigma_{l\nu}$ are both linear in T, neglecting $\delta\sigma_s$ causes ΔC_3 to be overestimated, but does not degrade the quality of the fit. By itself the prewetting line data gives no insight into $\delta\sigma_s$. The prewetting step height offers a check of ΔC_3. Intrinsic to the derivation of Eq. (2) is a relation between the step height, d, and $\Delta\mu$: $d = (\Delta C_3/\Delta\mu)^{1/3}$. Using $\Delta C_3 = 1800$ K Å^3 gives the solid line in Fig. 4. The fit is acceptable, but because of the cube root, this check on the value of ΔC_3 is not particularly sensitive.

The value of T_W is smaller than the most recent theoretical prediction of 22 K.[13] Taking a value of 900 K Å^3 for $C_3^{\mathrm{H}_2}$ (Ref. 2) and our value for ΔC_3 gives 2700 ± 300 K Å^3 for C_3^{Cs}, somewhat smaller than the theoretical value of 3300 K Å^3.[13] The most striking result of our experiment is the temperature dependence of $\delta\sigma_s$ which is not constant but varies at fully $\frac{1}{3}$ the rate of $\sigma_{l\nu}$.

---

*Present address: Ecole Normale Superieure, Laboratoire de Physique Statistique, 24 rue Lhomond, Paris cedex 05, France.

[1] E. Cheng, G. Mistura, H. C. Lee, M. H. W. Chan, M. W. Cole, C. Carraro, W. F. Saam, and F. Toigo, Phys. Rev. Lett. **70**, 1854 (1993).

[2] G. Mistura, H. C. Lee, and M. H. W. Chan, J. Low Temp. Phys. **96**, 221 (1994).

[3] G. B. Hess, M. J. Sabatini, and M. H. W. Chan, Phys. Rev. Lett. **78**, 1739 (1997).

[4] E. Cheng, M. W. Cole, W. F. Saam, and J. Treiner, Phys. Rev. Lett. **67**, 1007 (1991).

[5] M. S. Pettersen and W. F. Saam, Phys. Rev. B **51**, 15 396 (1995).

[6] W. F. Saam, J. Treiner, E. Cheng, and M. W. Cole, J. Low Temp. Phys. **89**, 637 (1992).

[7] J. E. Rutledge and P. Taborek, Phys. Rev. Lett. **69**, 937 (1992).

[8] D. Ross, J. E. Rutledge, and P. Taborek, Science **278**, 664 (1997).

[9] D. Ross, P. Taborek, and J. E. Rutledge, J. Low Temp. Phys. **111**, 1 (1998).

[10] R. E. Johnson and R. H. Dettre, in *Wettability*, edited by J. C. Berg (Dekker, New York, 1983), pp. 1–73.

[11] P. Clark Souers, *Hydrogen Properties for Fusion Energy* (University of California Press, Berkeley, CA, 1986).

[12] W. H. Press, S. A. Teukolsky, W. T. Vetterling, and B. P. Flannery, *Numerical Recipes* (Cambridge University Press, Cambridge, 1986).

[13] A. Chizmeshya, M. W. Cole, and E. Zaremba, J. Low Temp. Phys. **110**, 677 (1998).